MODELING BUBBLY-CAP FLOWS USING TWO-GROUP AVERAGE BUBBLE NUMBER DENSITY

G.H. Yeoh^{1,2}, S.C.P. Cheung³, J.Y. Tu³, E. Krepper⁴ and D. Lucas⁴

Australian Nuclear Science and Technology Organisation (ANSTO),

Locked Bag 2001, Kirrawee DC, NSW 2232 Australia

School of Mechanical and Manufacturing Engineering,

University of New South Wales, Sydney, NSW 2052, Australia

School of Aerospace, Mechanical and Manufacturing Engineering,

RMIT University, Victoria 3083, Australia

Institute of Safety Research, Forschungszentrum Rossendrof e.V.,

P.O. Box 510 119, 01314 Dresden, Germany

Abstract

The basic concept of two-group average bubble number density equations along with three-fluid model has been demonstrated for vertical gas-liquid flow. Specifically, the current study focused on: (i) classification of bubble interaction between spherical bubbles (Group-1) and cap bubbles (Group-2), (ii) preliminary consideration of source and sink terms in the averaged bubble number density equations via the model of Hibiki and Ishii [1] and (iii) assessment by means of experimental data sets at bubbly-to-cap flow transition. Reasonable agreement was achieved between measured and predicted distributions of void fraction, interfacial area concentration (IAC) and volume equivalent bubble diameter.

Introduction

Many challenges remain in the development of physical models for gas-liquid flow. Based on the consideration of the interpenetrating media approach, the inter-phase exchanges of mass, momentum and energy can be modelled as interfacial transfer terms acting on each phase. In this sense, two sets of conservations (one conservation equation for mass, momentum and energy of the gas phase as well as liquid phase) are written in terms of phase-averaged properties. The dynamics of the interaction between the two phases are fully described by the constitutive relationships governing the inter-phase mass, momentum and energy exchange. Generally, these interfacial transfer terms comprise the IAC or bubble size. In order to properly solve these two sets of conservation equations, the local IAC or bubble size needs to be determined through suitable mechanistic models accounting for the physical interaction between the two phases and the gradual transition between the different flow regimes.

Appropriate models for IAC through the use of flow regime maps are generally adopted in the absence of any alternative models. Nevertheless, flow pattern maps do not account for the time and length scale for the flow regime transition between two flow regimes and arbitrarily smoothing function at the boundary between the two flow regimes are employed instead to avoid numerical instabilities. These features have certainly driven the interfacial structure to be less physical. Therefore, greater emphasis must be refocused in the development of mechanistic models to account for the physical interaction between the two phases and the gradual transition between the different

flow regimes. To achieve this, more physical insights into the processes that lead to the characterization of the interfacial transport phenomena in different flow regimes are required.

The transport phenomena of dispersed bubbles in bubbly flow conditions can be regarded in a similar view of the drag and interaction mechanisms of spherical bubbles. Most coalescence and break-up mechanisms have been principally based on the assumption of interaction between spherical bubbles [2-7]. Nevertheless, cap bubbles that are precursors to the formation of slug units in the slug flow regime as well as the accumulation of large unsteady gas volumes within these mixing regions which produce the churn-turbulent flow regime with increasing volume fraction become ever more prevalent at high gas velocity conditions. Experiments have shown that the interaction behaviours between non-spherical bubbles in the liquid flow are generally different when compared against to those of spherical bubbles; additional mechanisms of bubble interactions are thus required.

Focusing on the intra-group mechanisms of spherical bubbles, the usual coalescence and break-up processes due to random collisions and turbulent impact have been considered. The intra-group mechanisms for non-spherical bubbles take however a more complex consideration where the bubble coalescence may be due to random collisions and wake entrainment while the bubble break-up may be attributed by turbulent impact and possibly shearing-off as well as surface instability [8]. In addition to intra-group interactions, it has also been demonstrated through Hibiki and Ishii [1] that the inter-group interactions may also contribute significantly to the transport of the interfacial states, which principally govern the dominant mass transfer between the spherical and non-spherical bubbles. Similar mechanisms from the above considerations for intra-group interactions may be taken for inter-group interactions.

In this paper, the modelling framework that includes the classification of bubbles of different sizes and shapes into different groups entails the consideration of additional transport equations to aptly describe the transport phenomena of these distinct groups [9]. Through the two-group averaged bubble number density equations and three-fluid model, the numerical predictions are evaluated against the experimental data for vertical, upward, air-water two-phase flows in medium and large diameter pipes undergoing various flow regimes.

1. Formulation of two-group model

1.1 Two-group average bubble number density equation

In gas-liquid flow, a wide range of bubble shapes and sizes exist depending on the given flow regime. The average bubble number density equation needs to describe the bubble transport in a wide range of two-phase flow regimes, accounting for the differences in the transport characteristics of different types of bubbles. Due to the markedly different drag forces as well as bubble interaction mechanisms, the two-group formulation necessitates the treatment of bubbles into two distinct groups, namely Group-1 bubbles consisting of spherical bubbles and Group-2 bubbles consisting of cap bubbles. The Group-1 bubbles exist in the range of minimum bubble size to the maximum distorted bubble diameter as suggested by Ishii and Zuber [10]:

$$D_{d,max} = 4\sqrt{\frac{\sigma}{g\Delta\rho}} \tag{1}$$

whereas Group-2 bubbles exist in the range of the above limit to some maximum stable size limit:

$$D_{max} = 40\sqrt{\frac{\sigma}{g\Delta\rho}} \tag{2}$$

The foundation of the average number density equation stems from the Boltzmann transport equation, which describes the particle transport by an *integro-differential* equation of the particle size distribution function. In general, the particle transport equation is much too detailed to be employed in practice; it is therefore averaged over all particle sizes for practical application. Hence, the two-group average bubble number density transport equations can be obtained by averaging the particle transport equation over the volume range of each bubble group; *viz.*,

$$\frac{\partial n_1}{\partial t} + \nabla \cdot \left(\vec{v}_1^g \ n_1 \right) = \sum_j \left(R_{j,1} + R_{j,12} \right) \tag{3}$$

$$\frac{\partial n_2}{\partial t} + \nabla \cdot \left(\vec{v}_2^g \, n_2 \right) = \sum_j \left(R_{j,2} + R_{j,21} \right) \tag{4}$$

where n is the average bubble number density and \bar{v}^g is the gas velocity. Note that the two-group average bubble number density equation is simplified to a one-group average bubble number density equation in the bubbly flow regime. As can be seen in equations (3) and (4), the source and sink terms must be specified via constitutive relations, which are exemplified in the next section.

1.2 Bubble mechanistic models

Possible interactions of the two-group bubbles based on the classification by Hibiki and Ishii [1] which are accounted through the source and sink terms in equations (3) and (4) are illustrated in Figure 1.

For the intra-group and inter-group mechanisms of Group-1 bubbles, the source and sink terms in equation (3) are:

$$\sum_{j} \left(R_{j,1} + R_{j,12} \right) = \underbrace{\phi_{1}^{RC} + \phi_{1}^{TI} + \phi_{12}^{WE}}_{intra-group} + \underbrace{\phi_{12}^{TI}}_{inter-group} + \underbrace{\phi_{12}^{TI}}_{inter-group}$$
(5)

where ϕ_1^{RC} , ϕ_1^{TI} and ϕ_{12}^{WE} are the bubble number density changes due to random collision, turbulent induced breakage and wake entrainment. In Hibiki and Ishii [1], the interactions between the two groups as well as sink and source terms in Group-2 bubbles have been omitted which result in only the intra-group mechanisms of Group-2 bubbles; the source and sink terms in equation (4) reduce to:

$$\sum_{j} \left(R_{j,2} \right) = \underbrace{\phi_2^{WE} + \phi_2^{TI}}_{intra-group} \tag{6}$$

The 14th International Topical Meeting on Nuclear Reactor Thermalhydraulics, NURETH-14 Toronto, Ontario, Canada, September 25-30, 2011

	Group-1	Inter-group	Group-2
Coalescence	Random collision	Wake entrainment	Wake entrainment
Breakup		Turbulent impa	ct

Figure 1 Schematic illustration of two-group bubble interactions [1].

Considering the intra-group mechanisms of Group-1 bubbles, the bubble random collision is approximated by assuming the bubble movement analogous to ideal gas molecules in an isotropic turbulence system. Using kinetic theory, the coalescence rate due to turbulent random collision is determined as:

$$\phi_{1}^{RC} = -\gamma_{1}^{RC} \frac{\left(\alpha_{1}^{g}\right)^{2} \left(\varepsilon^{l}\right)^{1/3}}{D_{b,1}^{11/3} \left(\alpha_{RC,\text{max}} - \alpha^{g}\right)} \times \exp\left(-K_{1}^{RC} \frac{D_{b,1}^{5/6} \left(\rho^{l}\right)^{1/2} \left(\varepsilon^{l}\right)^{1/3}}{\sigma^{1/2}}\right)$$
(7)

where γ_1^{RC} and K_1^{RC} are adjustable constants and $\alpha^g = \alpha_1^g + \alpha_2^g$. The break-up rate can also be derived according to the kinetic theory, which is correlated to the frequency for a given bubble colliding with the turbulent eddy as:

$$\phi_{1}^{TI} = \gamma_{1}^{TI} \frac{\alpha_{1}^{g} (1 - \alpha_{1}^{g}) (\varepsilon^{l})^{1/3}}{D_{b,1}^{11/3} (\alpha_{TI, \max} - \alpha^{g})} \exp \left(-K_{1}^{TI} \frac{\sigma}{\rho^{l} D_{b,1}^{5/3} (\varepsilon^{l})^{2/3}} \right)$$
(8)

where γ_1^{TI} and K_1^{TI} are adjustable constants.

For the inter-group mechanisms Group-1 bubbles, the model of wake entrainment induced bubble coalescence has been proposed by Hibiki and Ishii [1] for the collision between spherical and cap bubbles. In the model, it has been assumed that all bubbles in the wake region collide with the leading cap bubble, which is approximated to be a large spherical bubble with the equivalent volume of the cap bubble. The coalescence rate due to wake entrainment is expressed as:

The 14th International Topical Meeting on Nuclear Reactor Thermalhydraulics, NURETH-14 Toronto, Ontario, Canada, September 25-30, 2011

$$\phi_2^{WE} = -\gamma_{12}^{WE} \frac{\alpha_1^g \alpha_2^g}{D_{b,1}^3 D_{b,2}} \left(v_{axial,2} - v^l \right) \times \exp \left\{ -K_{12}^{WE} \frac{\left(\rho^l \right)^{1/2} \left(\varepsilon^l \right)^{1/3}}{\sigma^3} \left(\frac{D_{b,1} D_{b,2}}{D_{b,1} + D_{b,2}} \right)^{5/6} \right\}$$
(9)

where $v_{axial,2}$ and v^l define the cap bubble velocity in the axial direction and liquid velocity of the fluid flow while γ_{12}^{WE} and K_{12}^{WE} are adjustable constants. In equation (9), the coalescence efficiency of two bubbles of different sizes has been realized using the equivalent diameter proposed by Chesters and Hoffmann [11]. In a similar way to the break-up rate for Group-1 bubbles, the break-up rate for ϕ_{12}^{TI} can be correlated to the frequency of the collision between the turbulent eddy and the bubble according to:

$$\phi_{12}^{TI} = \gamma_{12}^{TI} \frac{\alpha_2^g \left(1 - \alpha^g\right) \left(\varepsilon^l\right)^{1/3}}{D_{b,2}^{11/3} \left(\alpha_{TI,\text{max}} - \alpha^g\right)} \times \exp\left(-K_{12}^{TI} \frac{\sigma \left\{D_{b,2}^3 - D_{b,1}^3\right)^{2/3} + \left(D_{b,1}^2 - D_{b,2}^2\right)\right\}}{\rho^l D_{b,2}^{11/3} \left(\varepsilon^l\right)^{2/3}}\right)$$
(10)

where γ_1^{TI} and K_1^{TI} are adjustable constants. The expression in equation (10) has been derived based on the break-up of a cap bubble into a smaller cap bubble and a spherical bubble.

Finally, the intra-group mechanisms of Group-2 bubbles can be obtained from analogous considerations of wake entrainment and turbulent impact as aforementioned. The coalescence rate due to wake entrainment is given by:

$$\phi_2^{WE} = -\gamma_2^{WE} \frac{\left(\alpha_2^g\right)^2}{D_{b,2}^4} \left(v_{axial,2} - v^l\right) \times \exp\left\{-K_2^{WE} \frac{D_{b,2}^{5/6} \left(\rho^l\right)^{1/2} \left(\varepsilon^l\right)^{1/3}}{\sigma^{1/2}}\right\}$$
(11)

while the break-up rate due to turbulent impact is obtained from:

$$\phi_{2}^{TI} = \gamma_{2}^{TI} \frac{\alpha_{2}^{g} \left(1 - \alpha^{g}\right) \left(\varepsilon^{l}\right)^{1/3}}{D_{b,2}^{11/3} \left(\alpha_{TI,\text{max}} - \alpha^{g}\right)} \exp\left(-K_{2}^{TI} \frac{\sigma}{\rho^{l} D_{b,2}^{5/3} \left(\varepsilon^{l}\right)^{2/3}}\right)$$
(12)

where γ_2^{WE} , γ_2^{TI} , K_2^{WE} and K_2^{TI} are adjustable constants. The expression in equation (12) has been derived based on the break-up of a cap bubble into two smaller cap bubbles. More details regarding the specific formulation of the above mechanisms can be referred in Hibiki and Ishii [1].

2. Three-fluid model

Generally, the pressure and temperature for Group-1 and Group-2 bubbles can be assumed to be approximately the same. However, the velocities of the two groups cannot be taken to flow at a common velocity. Therefore, it is necessary that additional transport equations for the conservation of mass and momentum are introduced. On the basis of the above assumption, the density of the gas phase is the same for Group-1 and Group-2 bubbles. The ensemble-averaged equations for the conservation of mass for the gas phase are thus given by.

The 14th International Topical Meeting on Nuclear Reactor Thermalhydraulics, NURETH-14 Toronto, Ontario, Canada, September 25-30, 2011

$$\frac{\partial \left(\rho^{g} \alpha_{1}^{g}\right)}{\partial t} + \nabla \cdot \left(\rho^{g} \alpha_{1}^{g} \bar{v}_{1}^{g}\right) = -\dot{m}_{12} \tag{13}$$

$$\frac{\partial \left(\rho^{g} \alpha_{2}^{g}\right)}{\partial t} + \nabla \cdot \left(\rho^{g} \alpha_{2}^{g} \vec{v}_{2}^{g}\right) = \dot{m}_{12} \tag{14}$$

where \dot{m}_{12} represents the inter-group mass transfer due to coalescence and break-up effects. The ensemble-averaged equations for the conservation of momentum of Group-1 and Group-2 bubbles become:

$$\frac{\partial \left(\rho^{g} \alpha_{1}^{g} \vec{v}_{1}^{g}\right)}{\partial t} + \nabla \cdot \left(\rho^{g} \alpha_{1}^{g} \vec{v}_{1}^{g} \vec{v}_{1}^{g}\right) = -\alpha_{1}^{g} \nabla P + \alpha_{1}^{g} \rho^{g} \vec{g} + \nabla \cdot \left[\alpha_{1}^{g} \left(\mu^{g} + \mu_{T}^{g}\right) \left(\nabla \vec{v}_{1}^{g} + \left(\nabla \vec{v}_{1}^{g}\right)^{T}\right) - \dot{m}_{12} \vec{v}_{1}^{g} + F_{1}^{gl}\right]$$
(15)

$$\frac{\partial \left(\rho^{g} \alpha_{2}^{g} \vec{v}_{2}^{g}\right)}{\partial t} + \nabla \cdot \left(\rho^{g} \alpha_{2}^{g} \vec{v}_{2}^{g} \vec{v}_{2}^{g}\right) = -\alpha_{2}^{g} \nabla P + \alpha_{2}^{g} \rho^{g} \vec{g} + \nabla \cdot \left[\alpha_{2}^{g} \left(\mu^{g} + \mu_{T}^{g}\right) \left(\nabla \vec{v}_{2}^{g} + \left(\nabla \vec{v}_{2}^{g}\right)^{T}\right)\right] + \dot{m}_{12} \vec{v}_{2}^{g} + F_{2}^{gl}$$
(16)

For the liquid phase, the ensemble-averaged equations for conservation of mass and momentum can be written as:

$$\frac{\partial \left(\rho^{l} \alpha^{l}\right)}{\partial t} + \nabla \cdot \left(\rho^{l} \alpha^{l} \vec{v}^{l}\right) = 0 \tag{17}$$

$$\frac{\partial \left(\rho^{l} \alpha^{l} \vec{v}_{l}^{l}\right)}{\partial t} + \nabla \cdot \left(\rho^{l} \alpha^{l} \vec{v}^{l} \vec{v}_{l}^{l}\right) = -\alpha^{l} \nabla P + \alpha^{l} \rho^{l} \vec{g} + \nabla \cdot \left[\alpha^{l} \left(\mu^{l} + \mu_{T}^{l}\right) \left(\nabla \vec{v}_{1}^{l} + \left(\nabla \vec{v}_{1}^{l}\right)^{T}\right)\right] + F_{1}^{lg} + F_{2}^{lg}$$
(18)

The total interfacial forces F_1^{lg} (Group-1) and F_2^{lg} (Group-2) appearing in equation (15) are formulated according to appropriate consideration of different sub-forces affecting the interface between each phase. As demonstrated by Frank et al. [12], the total interfacial forces for the respective groups of bubbles are given by the drag, lift, wall lubrication and turbulent dispersion, viz.

$$F_1^{lg} = -F_1^{gl} = F_{1,drag}^{lg} + F_{1,lif}^{lg} + F_{1,wall\ lubrication}^{lg} + F_{1,trbulent\ dispersion}^{lg}$$
(19)

$$F_2^{lg} = -F_2^{gl} = F_{2,drag}^{lg} + F_{2,lift}^{lg} + F_{2,wall\ lubrication}^{lg} + F_{2,turbulent\ dispersion}^{lg}$$

$$(20)$$

In equations (19) and (20), appropriate relationships of the drag, lift, wall lubrication and turbulent dispersion forces are described based on the formulations of Ishii and Zuber [10], Drew and Lahey [13], Antal et al. [14] and Burns et al. [15]. For bubbly-cap flow, the drag coefficient for Group-1

bubbles is correlated for several distinct Reynolds number regions for individual bubbles according to Ishii and Zuber [10]. Nevertheless, the drag coefficient for Group-2 bubbles can be approximated to be 8/3 [16]. The lift coefficient is determined via Tomiyama's [17] relationship – a function of the Eötvos number that allows positive and negative lift coefficients depending on the bubble size and also accounts for the effects of bubble deformation and asymmetric wake of the bubble. Suggested values by Krepper et al. [18] are employed for the wall lubrication constants.

In handling bubble induced turbulent flow, unlike single phase fluid flow problem, no standard turbulence model is tailored for gas-liquid flow. Following our previous studies [19], the Shear Stress Transport (SST) model which applies the two-equation k- ω model near the wall and the two-equation k- ε model in the bulk flow, is employed herein. To account for the effect of bubbles on liquid turbulence, the Sato's bubble-induced turbulent viscosity model is employed [20]. The dispersed phase zero equation model is utilized for the gas phase turbulent viscosity.

3. Experimental details

For the medium diameter pipe, two-phase flow experiments conducted by Hibiki et al. [21] were chosen to assess the two-group model in simulating the bubbly-cap flow region. The test section has a round tube made of acrylic with an inner diameter (D) of 50.8 mm and a length (L) of 3061 mm. The temperature of the apparatus was kept at a constant temperature of 20° C within the deviation of $\pm 0.2^{\circ}$ C. Local flow measurements using the double sensor and hot-film anemometer probes were performed at three axial (height) locations of z/D = 6.0, 30.3 and 53.5 and 15 radial locations of r/R = 0 to 0.95. A range of superficial liquid velocities and superficial gas velocities have been performed, which covered mostly the bubbly flow region, including finely dispersed bubbly flow and bubbly-to-slug transition flow regions. Area averaged superficial gas velocity j_g was obtained from local void fraction and gas velocity measured by the double sensor probe, whereas area averaged superficial liquid velocity j_f was obtained from local void fraction measured by the double sensor probe and local liquid velocity measured by the hot-film anemometry. More details regarding the experimental set-up can be referred in Hibiki et al. [21].

For the large diameter pipe, two-phase flow experiments performed at the TOPFLOW facility by Prasser et al. [22] were chosen to assess the two-group model in simulating the bubbly-cap flow region. The test section has a large size vertical cylindrical pipe with a length (L) of 9000 mm and inner diameter (D) of 195.3 mm inner diameter. Water was circulated from the bottom to the top with a constant temperature of 30°C, maintained by a heat exchanged installed in the water reservoir. A variable gas injection system was constructed by equipping with gas injection units at 18 different axial positions from z/D = 1.1 to 9.9. Three levels of air chambers were installed at each injection unit. The upper and the lower chambers have 72 annular distributed orifices of 1 mm diameter for small bubble injection while the central chamber has 32 annularly distributed orifices of 4 mm diameter for large bubble injection. A fixed wire-mesh sensor was implemented at the top of the pipe where instantaneous information of gas volume fraction as well as bubble size distribution was measured. More details regarding the experimental set-up can be found in Prasser et al. [22]

4. Results and discussion

Numerical calculations were achieved through the use of the generic computational fluid dynamics code ANSYS-CFX11. The average bubble number density transport equations with appropriate

source and sink terms describing the coalescence and break-up rate of bubble were implemented through the CFX Command Language (CCL). For the purpose of computational efficiency, radial symmetry was assumed so that the numerical simulations could be performed on a 60° radial sector of the pipe with symmetry boundary conditions at both sides. Inlet conditions were assumed to be homogeneous with regards to the superficial liquid and gas velocities, void fractions for both phases and uniformly distributed bubble size in accordance with the flow conditions described in Table 1. At the pipe outlet, a relative average static pressure of zero was specified. Three-dimensional meshes containing hexagonal elements were generated for the medium and large diameter pipe domains.

Cases	Superficial gas velocity [m/s]	Superficial water velocity [m/s]	Pipe diameter [m]	Experiments
1	0.321	0.986	0.0508	Hibiki et al. [21]
2	0.624	2.01	0.0508	
3	0.0574	1.017	0.1953	Prasser et al. [22]
4	0.0898	1.017	0.1953	

For cases 1 and 2, the prevalence of cap bubbles in the medium diameter pipe can be seen to be evident for higher gas superficial velocity such as indicated by the higher void fraction of Group-2 bubbles in Figure 1. Axial profiles of predicted area-averaged void fraction showed reasonable agreement with the measured data.

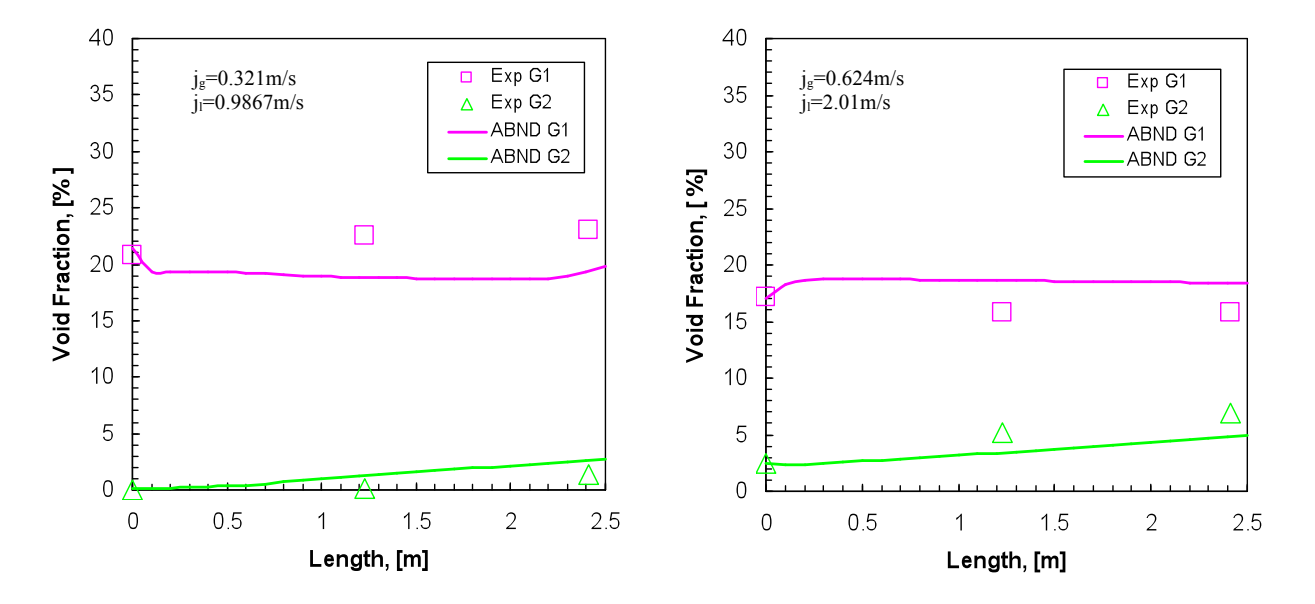


Figure 1 Evolution of measured and predicted void fraction profiles along axial direction with increasing superficial velocities jg and jf for cases 1 and 2.

Figure 2 illustrates the axial profiles of the volume equivalent bubble diameter of cases 1 and 2. Good agreement between the measured and predicted axial profiles of the volume equivalent bubble diameter of Group-1 bubbles (i.e. green line) indicated that the mechanisms governed by coalescence due to random collision driven by liquid turbulence and the break-up due to the impact of turbulent eddies were sufficient to capture the appropriate bubble interaction behaviours for spherical bubbles occurring within the two-phase flow. Nevertheless, the inability of the numerical model to predict the axial profiles of the volume equivalent bubble diameter of Group-2 bubbles (i.e. solid line) demonstrated the need for further insights and development of appropriate mechanisms to better capture the prevailing bubble interaction behaviours governing Group-2 bubbles.

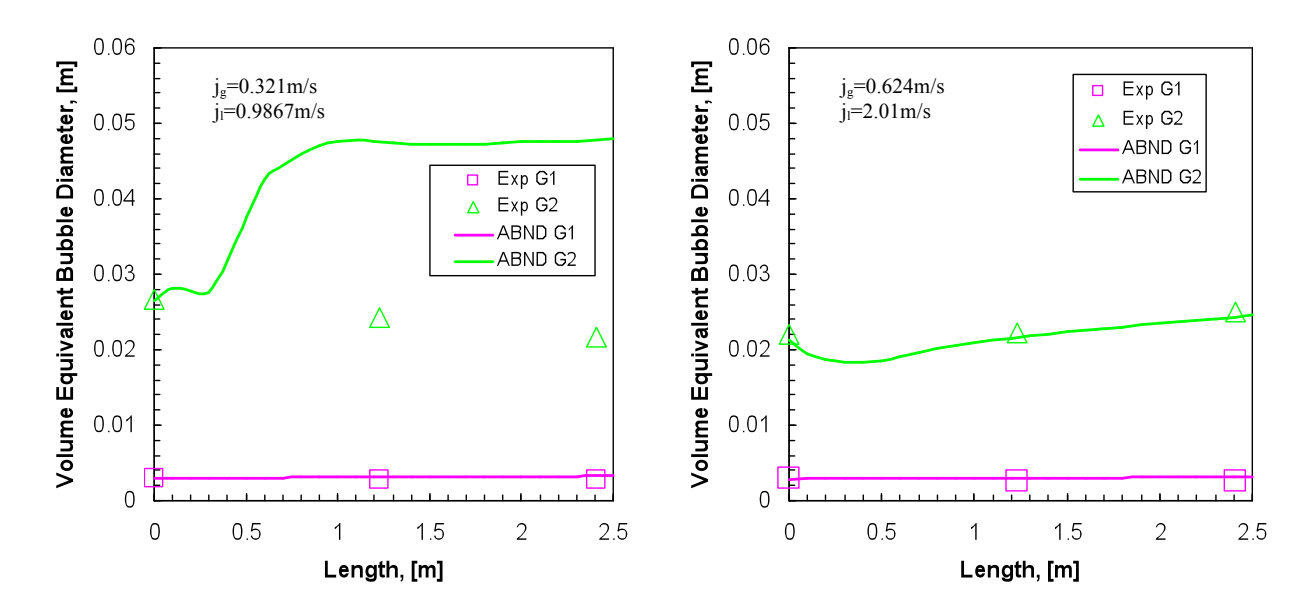


Figure 2 Evolution of measured and predicted volume equivalent diameter profiles along axial direction with increasing superficial velocities j_g and j_f for cases 1 and 2.

For cases 3 and 4, the prevalence of cap bubbles in the large diameter pipe can be seen to be evident near the inlet of the pipe such as indicated by the higher void fraction of Group-2 bubbles in Figure 3. Nevertheless, the decreasing trend of Group-2 bubbles illustrated the significant mass transfer occurring from Group-2 bubbles to Group-1 bubbles which was primarily effected through the intergroup mechanisms of bubble interaction governed by the break-up of cap bubbles due to the impact of turbulent eddies as the flow developed downstream along the vertical large pipe.

Figure 4 illustrates the axial profiles of the volume equivalent bubble diameter of cases 3 and 4. The axial profiles of the volume equivalent bubble diameter of Group-1 bubbles (i.e. dashed line) can be seen to be predicted rather well against the axial evolution of measured sizes. Similar to the case of the medium diameter pipe, the mechanisms governed by coalescence due to random collision driven by liquid turbulence and the break-up due to the impact of turbulent eddies were also prevalent to be sufficient to capture the appropriate bubble interaction behaviours for spherical bubbles occurring within the two-phase flow for the large diameter pipe. Nevertheless, the deficiency of numerical model in predicting the axial profiles of the volume equivalent bubble diameter of Group-2 bubbles (i.e. solid line) demonstrated again the need for further insights and development of appropriate mechanisms for Group-2 bubbles.

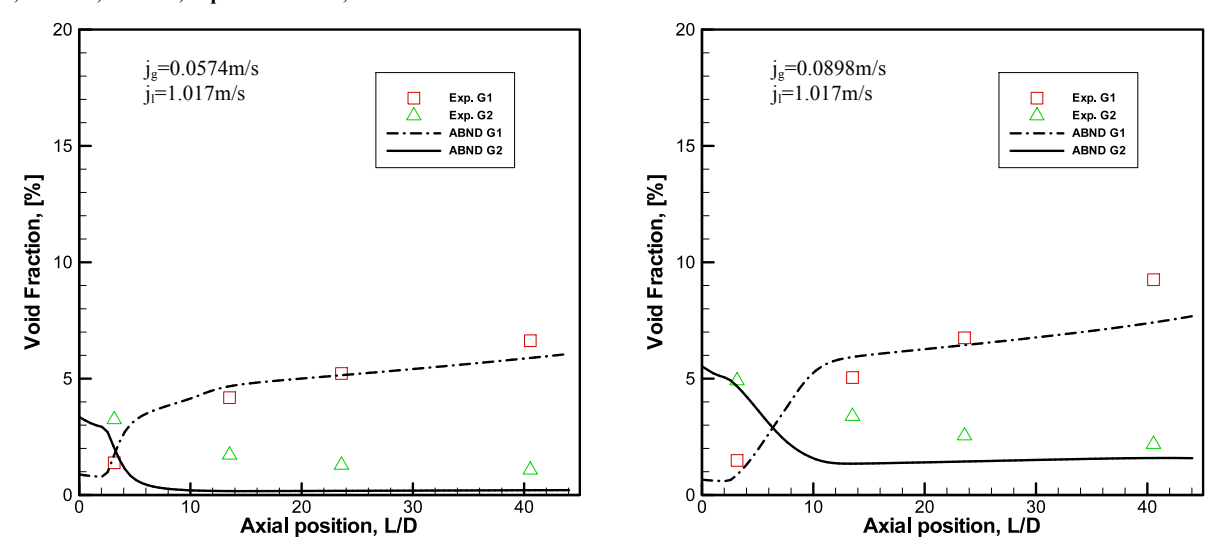


Figure 3 Evolution of measured and predicted void fraction profiles along axial direction with increasing superficial velocities j_g and j_f for cases 3 and 4.

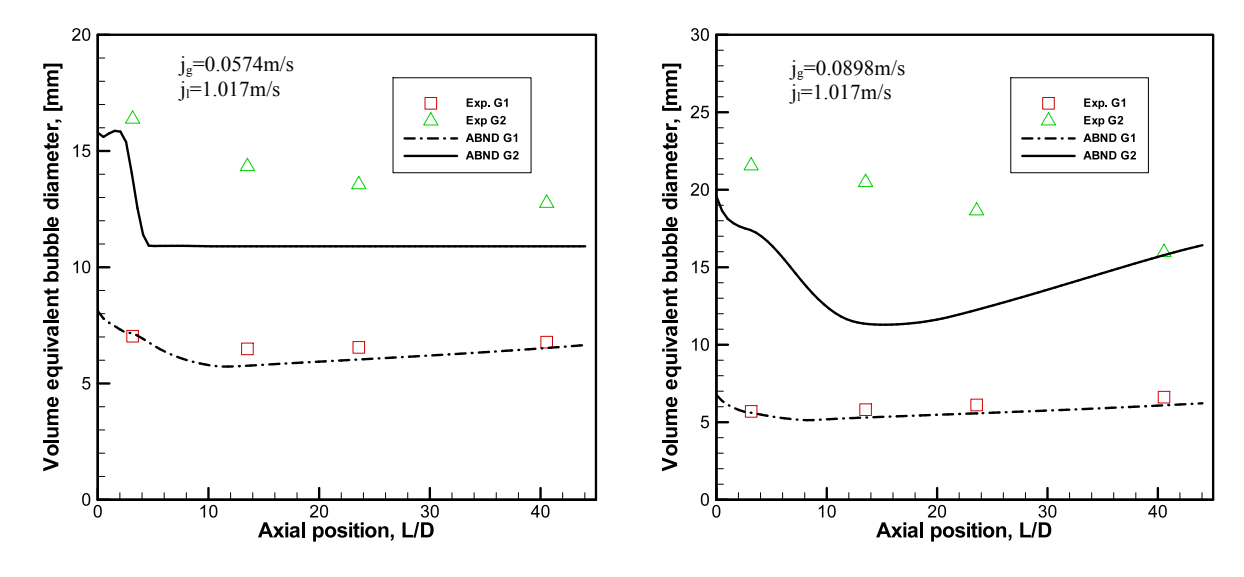


Figure 4 Evolution of measured and predicted volume equivalent diameter profiles along axial direction with increasing superficial velocities jg and jf for cases 3 and 4.

5. Conclusion

The two-group transport equations for the average bubble number density have been formulated by considering two groups of bubbles such as spherical bubbles being Group-1 and cap bubbles being Group-2. Based on the proposal of Hibiki and Ishii [1], possible interaction mechanisms for Group-1 and Group-2 bubbles have been utilized to close the equations. For Group-1 bubbles, the bubble interaction mechanisms of coalescence and break-up by considering bubble random collision and impact of turbulent eddies successfully predicted the local and axial distributions of void fraction, IAC and volume equivalent bubble diameter. For flow conditions where the void fractions are lower than about 20%, the one-group transport equation for the average bubble number density could be applied as the flow is mainly dominated by Group-1 bubbles. The two-group transport equations for the average bubble number density have been introduced to explain the interfacial transport phenomena at the bubbly-to-cap flow transition. Preliminary assessment on the bubble interaction

mechanisms of coalescence and break-up by considering random collision, wake entrainment and turbulent impact has been performed. The predicted results showed that the significant coalescence and break-up between Group-1 and Group-2 bubbles could be adequately captured via the intergroup mechanisms which yielded satisfactory mass transfer between these two groups of bubbles. Nevertheless, further insights and development of appropriate intra-group mechanisms to better capture the prevailing bubble interaction behaviours governing Group-2 bubbles are still required. Overall, the initial utilization of the three-fluid model and two-group average bubble number density equations have shown to be promising in the prediction of interfacial transport in gas-liquid flow.

6. References

- [1] T. Hibiki and M. Ishii, "Two-group interfacial area transport equations at bubbly-to-slug flow transition", Nuc. Eng. Des., Vol. 202, 2002, pp. 39-76.
- [2] Q. Wu, S. Kim, M. Ishii, and S.G. Beus, "One-group interfacial area transport in vertical bubbly flow", Int. J. Heat Mass Transfer, Vol. 41, 1998, pp.1103-1112.
- [3] T. Hibiki and M. Ishii, "Development of One-group interfacial area transport equation in bubbly flow systems", Int. J. Heat Mass Transfer, Vol. 45, 2002, pp. 2351-2372.
- [4] W. Yao and C. Morel, "Volumetric interfacial area prediction in upwards bubbly two-phase flow", Int. J. Heat Mass Transfer, Vol. 47, 2004, pp. 307-328.
- [5] M.J. Prince and H.W. Blanch, "Bubble coalescence and break-up in air-sparged bubble column", AIChE J., Vol. 36, 1990, pp. 1485-1499.
- [6] H. Luo and H. Svendsen, "Theoretical model for drop and bubble break-up in turbulent dispersions", AIChE J., Vol. 42, 1996, pp. 1225-1233.
- [7] S. Lo and D.S. Zhang, "Modeling break-up and coalescence in bubbly two-phase flows, J. Comp. Multiphase Flows, Vol. 1, 2009, pp. 23-38.
- [8] X.D. Sun, S. Kim, M. Ishii and S.G. Beus, "Modeling of bubble coalescence and disintegration in confined upward two-phase flow", Nuc. Eng. Des., Vol. 230, 2004, pp. 3-26.
- [9] T. Hibiki and M. Ishii, "Interfacial area transport equations for gas-liquid flow", J. Comp. Multiphase Flows, Vol. 1, 2009, pp. 1-22.
- [10] M. Ishii and N. Zuber, "Drag coefficient and relative velocity in bubbly, droplet or particulate flows", AIChE J., Vol. 25, 1979, pp. 843-855...
- [11] A.K. Chesters and G. Hofman, "Bubble coalescence in pure liquids", Appl. Sci. Res., Vol. 38, 1982, pp. 353-361..
- [12] T. Frank, J. Shi and A.D. Burns, "Validation of Eulerian multiphase flow models for nuclear safety application", Proceedings of Third Symposium on Two-Phase Modeling and Experimentation, Pisa, Italy, 2004.
- [13] D.A. Drew and R.T.Jr. Lahey, "Application of general constitutive principles to the derivation of multi-dimensional two-phase flow equation", Int. J. Multiphase Flow, Vol. 5, 1979, pp. 243-264.

- [14] S.P. Antal, R.T.Jr. Lahey and J.E. Flaherty, "Analysis of phase distribution and turbulence in dispersed particle/liquid flows", Chem. Eng. Comm., Vol. 174, 1991, pp. 85-113.
- [15] A.D. Burns, I. Hamill, T. Frank and J. Shi, "The Favre averaged drag model for turbulent dispersion in Eulerian multiphase flow", Fifth International Conference on Multiphase Flow, Yokohama, Japan, 2004.
- [16] A. Tomiyama, I. Kataoka and T. Sakaguchi, "Drag coefficients of bubbles (1st report, drag coefficients of a single bubble in a stagnant liquid)", Trans. JSME, Vol. 61, 1995, pp. 2357-2364.
- [17] E. Krepper, D. Lucas and H. Prasser, "On the modeling of bubbly flow in vertical pipes", Nuc. Eng. Des., Vol. 235, 2005, pp. 597-611.
- [18] A. Tomiyama, "Struggle with computational bubble dynamics", Third International Conference on Multiphase Flow, Lyon, France, 1998.
- [19] S.C.P. Cheung, G.H. Yeoh and J.Y. Tu, "On the numerical study of isothermal bubbly flow using two population balance approaches", Chem. Eng. Sci., Vol. 31, 2007, pp. 164-1072.
- [20] T. Sato, M. Sadatomi and K. Sekoguchi, "Momentum and heat transfer in two-phase bubbly flow-I", Int. J. Multiphase Flow, Vol. 7, 1981, pp. 167-178.
- [21] T. Hibiki, M. Ishii, Z. Xiao, "Axial interfacial area transport of vertical bubbly flows", Int. J. of Heat and Mass Transfer, Vol. 44, 2001, pp. 1869-1888.
- [22] H.M. Prasser, M. Beyer, H. Carl, S. Gregor, D. Lucas, H. Pietruske, P. Schutz and F.P. Weiss, "Evolution of the structure of a gas-liquid two-phase flow in a large vertical pipe", Nuc. Eng. Des., Vol. 237, 2007, pp. 1848-1861.